Wiley
Advances in Civil Engineering
Volume 2024, Article ID 3460968, 18 pages
https://doi.org/10.1155/2024/3460968

WILEY

Research Article

The Use of Transition Curves in Airport Runway Rapid Exit Taxiways (RETs)

Donato Ciampa, Maurizio Diomedi, Pietro Vuono, and Saverio Olita

School of Engineering, University of Basilicata, Potenza 85100, Italy

Correspondence should be addressed to Donato Ciampa; donato.ciampa@unibas.it

Received 4 March 2024; Revised 26 August 2024; Accepted 5 September 2024

Academic Editor: Zeybek Mustafa

This paper describes a study result focused on the transition curves used in airport rapid exit taxiways (RETs). Such geometric elements are not currently made explicit by standards, and major international government agencies, such as the International Civil Aviation Organization and the Federal Aviation Administration, are limited to providing some layouts consisting of only constant curvature elements, although the aircrafts speed in RETs is variable. In addition to the clothoid that has unitary shape parameter "*n*" and the multiparameter clothoids (generalized Cornu spirals), the study analyzes the Bloss curve employment. Regarding the multiparameter clothoids, four schemes with shape parameter equal to 1.25, 1.50, 1.75, and 2.00 were considered, respectively. The proposed curves' effectiveness was evaluated by analyzing the main geometric and kinematic variables trend, that is, curvature, transversal acceleration, lateral jerk, speed, travel time, longitudinal deceleration, and centrifugal force. To ensure the analysis effectiveness, the study layouts were designed from those used for runways codes 1-2 and 3-4 maintaining the main geometric elements dimensions unchanged (length of straight lines, radii of circular curves, exit angles, etc.). The kinematic variables values along the design RETs were calculated "point by point" by MATLAB software to take into account nonuniform motion regimen. The obtained results show that both the Bloss curve and the multiparameter clothoid having a shape factor equal to 2 are capable of better contribution in terms of safety and comfort. Implications in the airport construction field are related to the possibility of using lower deceleration values compared to current standards, that is, allowing higher exit speed for the same deceleration. This allows aircrafts to vacate the runway more quickly and, therefore, to increase runway capacity without taking expensive RETs repositioning.

1. Introduction

Rapid exit taxiways (RETs) make it possible to reduce the runway occupancy times (ROTs) of landing aircrafts and, thus, increase runways capacity [1]. By 2041, global passenger traffic is expected to reach 19.3 billion and airports will handle almost 200 million tons of air cargo worldwide [2]. In order to meet the growing mobility demand while ensuring limited travel time, comfort, and safety need to define and implement specific actions to make the planimetric layouts of RETs proposed by major government agencies, such as the International Civil Aviation Organization (ICAO) [3] and the Federal Aviation Administration (FAA) [4], more efficient.

From an operative point of view, it is recommended that such actions should be minimally invasive, limited to the geometric design, and such that they do not require the RETs repositioning along the runways [5] although it is known that the last factor significantly influence the ROTs values [6]. This is in order to avoid expensive and unpracticable retrofitting processes.

ICAO requires RETs when peak-hour traffic density is greater than a maximum value of 25 (landings and takeoffs) [7], while the FAA indicates a limit of 30 [8]. The handling of so many operations may generate a significant decrease in runway capacity. To avoid this decrease, it is necessary that operations be accomplished in the shortest time and that is generally achieved by increasing/decreasing aircraft speed/deceleration values. However, this also increases the accidents risk, such as collisions or runway excursions (veer-off risk) due to the generation of incorrect exit paths [9]. Veer-off is usually caused by pilot errors, incorrect speed/deceleration values, and/or the nonoptimal RETs geometry in terms of

exit angles, type, and succession of planimetric elements, radii of curvature, length of straight lines, etc. [10, 11].

Further risk factors are associated with approach speed and aircraft landing weight, friction conditions of runways and taxiways, type of aircraft, meteorological conditions, etc.

From the two ICAO reference layouts [7] adopted in almost all worldwide airports, the authors propose to explicitly insert between the constant curvature elements (initial straight line and circular curve), a variable curvature element (transition curve). This is in order to increase the system efficiency in terms of runway capacity and, at the same one time, to increase safety and travel comfort.

In fact, it is well-known that aircraft during taxiing perform as ground vehicles and as such, in the variable speed motion regimen that is characteristic of RETs, can take great kinematic benefits by transition curves usage [12].

Historically, this requirement has been pursued by the use of compound curves, which are circular curves having different radii located in succession. The first studies were conducted by Horonjeff et al. [13] in the late 1950s and were subsequently used by major government agencies in developing reference regulations. These studies were done on rigid and flexible pavements, both wet and dry, using different types of civil and military aircrafts. This was in order to evaluate the optimal relationship between exit speed, radii of curvature, and general configuration of RETs. Experimental tests showed that, at high speeds, the aircrafts followed paths are spirals, and this justified the use of compound curves given that, these curves approximate their geometry. In this sense, the central (or main) curve of R_2 radius should always be preceded by a circular curve of much larger radius R_1 [1].

In 1970, the FAA developed the first standards for RETs design and sizing with exit angles equal to 30° and 45° [14]. More specifically, for exit angles of 30°, these standards were required a circular curve with radius equal to 1800 feet (about 550 m) and a speed of 60 mph (about 96 km/h). For smaller aircraft, however, an exit angle equal to 45°, a radius of curvature of 800 feet (about 244 m) and a speed of 40 mph (about 64 km/h) were fixed. These layouts, therefore, did not consider the "explicit" use of compound curves in the first part of exit paths. Such use was later mandated by ICAO, which, in 1977, introduced a second radius of curvature [13, 14]. Currently, the use of compound curves and/or transition curves (widely used in road and rail engineering particularly if the travel speed is not constant) [15–19] is not explicitly provided in the airport field. This consideration is actually not rigorously true because the ICAO RETs layouts show a geometric offset equal to 0.90 m between the runway center line and the entry straightway for a length equal to 30 or 60 m before the circular curve [7]. Specifically, ICAO simply clarifies that the aforementioned offset (also known as shift factor), serves to "… facilitate pilot recognition of the beginning of the curve."

However, the authors point out that, from a geometric point of view, abovementioned offset has another important role, namely allowing the pilot to leave the runway center line and approach to the RET. The aircraft path followed in this "transition" zone, as already mentioned, is defined by a spiral [13] that can be reasonably substituted, in addition to a compound curve, by a variable radius transition curve that belongs to the same family of multiparameter clothoids (generalized Cornu spirals [GCS]) [12, 19].

This means that the ICAO layouts of RETs include a transition curve that is not geometrically defined [20].

In this study, the authors propose to make explicit the use of transition curves in the RETs and to define their paths using runway/taxiway center line marking [7, 21, 22]. So, the authors propose to integrate/modify the two ICAO layouts used in the airports that have runways codes 1-2 and 3-4 [7], respectively. These layouts are currently used in all 193 ICAO countries' member that represents almost all countries worldwide.

Historically, major government agencies such as the ICAO and FAA have not delved into the design of RETs from a geometric point of view. The considerations developed by the authors show that the geometric layout imposed by ICAO and FAA regulations are very basic and they are not fully efficient if travel speeds are widely variable. These government agencies have focused on studying the optimal location of RETs along runways in order to increase airport capacity. For example, the ICAO has implemented the so-called three-segment method [7] while the Virginia Tech (Project supported by the FAA) has developed the Runway Exit Design Interactive Model (REDIM software). Recently, however, even the FAA has realized the importance of improving the geometry of RETs and in fact, the latest version of the REDIM software (REDIM-V4) allows traditional schemes to be modified with the introduction of user-defined curves (https://atsl.cee.vt.edu/products.html). This work therefore contextualizes the need for the proposed geometric elements and the significance of the study.

Specifically, for each of the two abovementioned ICAO layouts, the authors propose and analyze six case studies generated by the use of the following types of transition curves: a clothoid with unitary "*n*" shape parameter (base case for comparison), four multiparameter clothoids with a shape parameter equal to 1.25, 1.50, 1.75, and 2.00 and a Bloss curve, also known as a biparametric or bihyperclothoid.

2. RETs

A RET is a taxiway connected to a runway so as to make an acute angle between their center lines. It allows landing aircrafts to leave the runway at higher speeds than are compatible with other types of exit taxiways, thus minimizing the ROT.

ICAO provides two geometric layouts for RETs design [7] depending on the runway code number [20]. The first layout (Figure 1) is used when the aeroplane reference field length (ARFL) is less than 800 m (runway code 1) or is between 800 and 1200 m excluded (runway code 2). The second one (Figure 2) is used when the ARFL is greater than 1200 m and less than 1800 m excluded (runway code 3) or is greater than 1800 m (runway code 4). The ARFL is defined as "the minimum field length required for take-off at maximum certificated take-off mass, sea level, standard atmospheric conditions, still air and zero runway slope, as shown in the appropriate airplane flight manual prescribed by the certificating authority or equivalent data from the airplane manufacturer" [7].

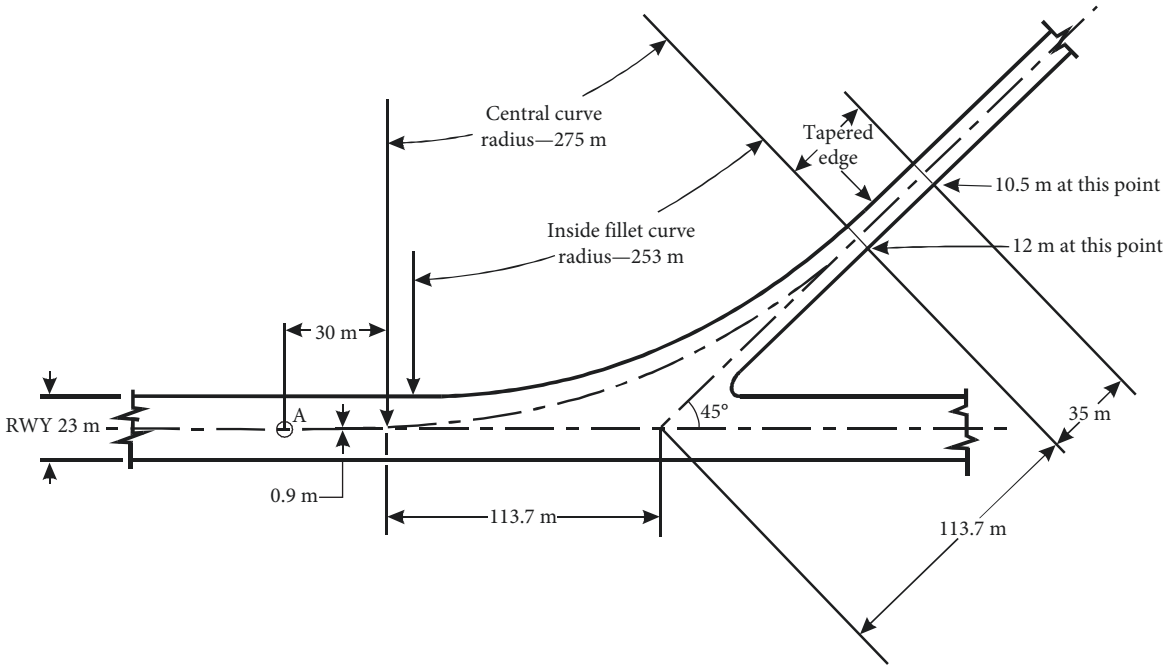

Figure 1: Rapid exit taxiway's ICAO layout used for codes 1 and 2 runways [7].

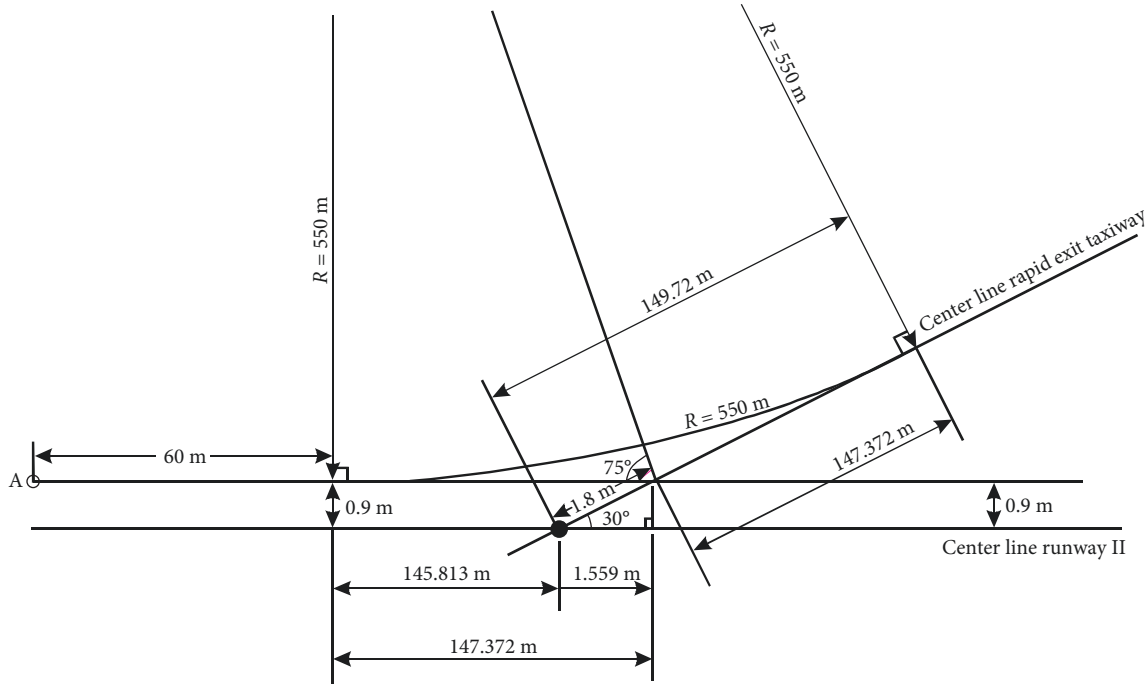

Figure 2: Rapid exit taxiway's ICAO layout used for codes 3 and 4 runways [7].

Establishing of a unified worldwide standard for RETs design is very relevant because in this manner pilots have got the same exit perception of runways at each airport.

The intersection angle between the RET's center line and the runways center line must not be greater than 45° or less than 25° and should more preferably be equal to 30° [7]. Particularly, 45° is assumed codes 1 and 2 runways and 30° in codes 3 and 4.

For runway codes 1 and 2, the taxiway center line marking starts at least 30 m before the tangency point of the central exit curve which has radius equal to 275 m and is offset by 0.9 m (Figure 1). For runway codes 3 and 4, it starts at least 60 m before the tangency point of the central exit curve which has radius equal to 550 m and is always offset by 0.9 m (Figure 2).

The maximum runway exit speed on wet pavement conditions is 93 km/h for runway codes 3 and 4 and 65 km/h for runway codes 1 and 2.

A RET should include a straight line after the turn-off curve long enough for an exiting aircraft to come to a full stop far from any intersecting taxiway. For this reason, both ICAO layouts include a final straight line which has a minimum length equal to 35 m (runway codes 1 and 2) and 75 m (runway codes 3 and 4) [7, 20].

These lengths are based on constant aircraft deceleration values assumed equal to 0.76 m/s^2 along the circular curve and 1.52 m/s^2 along the final straight line, respectively.

It should be noted that the FAA classifies the aircrafts into eight classes called taxiway design groups (TDGs) as a function of the various landing gear configurations. For each class, it suggests that the intersection angle between RETs and runways is always equal to 30° and the radius of the central exit curve is 457 m [21].

Also, FAA does not require the "explicit" use of compound curves or transition curves although, in the early 1990s, it introduced a 1400-foot (about 427 m) length spiral transition in the 30° exit layout [22]. However, this modification was definitively aborted in 2013.

3. Transition Curves

Below is a brief description of the main geometric and kinematic characteristics of the transition curves examined in this study, namely the clothoid, the multiparameter clothoid (GCS) and the Bloss curve. From a kinematic point of view, it is hypothesized that the speed v is constant. To take into consideration, the real motion conditions (uniformly variable motion regimen), kinematic checks will be developed "point by point" along the development of the transition curves.

It should be noted that the more detailed geometric explanation of these curves was developed by the authors in a previous road geometry study, to which reference is made for further details [23].

3.1. Clothoid. The clothoid is a curve having a variable radius used as a transition junction between elements having constant curvature. Its intrinsic equation in function of the scale factor "A" (in meters) shows a linear curvature trend ($1/r$) along the curvilinear abscissa (s), i.e. [12, 24, 25]:

$$r \times s = A^2. \tag{1}$$

The main relationships (in closed-form) which connect the variables previously described to the clothoid's final deviation angle t are as follows:

$$\tau = \frac{s^2}{2A^2} = \frac{s}{2r} = \frac{A^2}{2r^2}. \tag{2}$$

The Cartesian equation of the clothoid cannot be expressed in a closed-form, as can be observed from Expression (3):

$$\begin{cases} x = A\sqrt{2\tau} \cdot \sum_{i=1}^{\infty} (-1)^{i+1} \dfrac{\tau^{(2i-2)}}{(4i-3) \cdot (2i-2)!} \\ y = A\sqrt{2\tau} \cdot \sum_{i=1}^{\infty} (-1)^{i+1} \dfrac{\tau^{(2i-1)}}{(4i-1) \cdot (2i-1)!} \end{cases}. \tag{3}$$

For this work aims, it is need to analyze two important kinematic variables' trend along the curvilinear abscissa (variable from 0 to S), namely the transversal acceleration a_t and the lateral jerk c (variation of uncompensated transversal acceleration in the time). The analytical expressions of these kinematic quantities (with the obvious meaning of the symbols) are as follows:

$$a_t = \frac{v^2}{r} = \frac{v^2}{A^2} \cdot s, \tag{4}$$

$$c = \frac{da_t}{dt} = \frac{v^3}{A^2}, \tag{5}$$

where v is the (variable) aircraft speed, expressed in m/s.

It is useful to remember that the clothoid is completely efficient when the travel speed is constant and that, in this condition, transversal acceleration has a linear trend (Equation (4)), while lateral jerk stays constant (Equation (5)) [12].

A kinematic parameter that is evaluated in road construction is the rolling speed of the road platform. However, for RETs this parameter is not very significant because no lateral superelevation on curves is generally carried out [26].

In fact, you can see that ICAO, in order to calculate the radius of curves as a function of aircraft speed, assumes that the superelevation is zero and that the transverse friction value is very low (0.13) and speed independent [7, 26].

3.2. Multiparameter Clothoid (GCS). Multiparameter clothoids are transition curves that have a good attitude to be traveled at variable speed. They are identified by the following intrinsic equation [12, 24, 25, 27, 28]:

$$r \times s^n = A^{n+1}, \tag{6}$$

with obvious symbol significance, in which, the $n \neq 1$ variable is called shape parameter. This equation becomes the same as the clothoid if we impose $n = 1$ (Equation (1)).

Similar to the clothoid case (Equation (3)), the GCS Cartesian equation cannot be expressed in closed-form [12, 28]:

$$\begin{cases} x = A \cdot \sqrt[n+1]{(n+1) \cdot \tau} \cdot \left[\sum_{i=1}^{\infty} (-1)^{i+1} \dfrac{\tau^{(2i-2)}}{(2i-2)! \cdot p_i} \right] \\ y = A \cdot \sqrt[n+1]{(n+1) \cdot \tau} \cdot \left[\sum_{i=1}^{\infty} (-1)^{i+1} \dfrac{\tau^{(2i-1)}}{(2i-1)! \cdot q_i} \right] \end{cases}, \tag{7}$$

when:

$$\begin{cases} p_i = (2i-2)\cdot(n+1)+1 = 2in+2i-2n-1 \\ p_i = (2i-1)\cdot(n+1)+1 = 2in+2i-n \\ q_i = p_i + n + 1 \end{cases}. \tag{8}$$

Conversely, the variables τ, r, s, n, and A can be correlated with one another by closed relationships, as shown in the following equations [12, 28]:

$$r = \frac{A^{n+1}}{s^n} = \frac{A}{[(n+1)\cdot\tau]^{\frac{n}{n+1}}} = \frac{s}{(n+1)\cdot\tau}, \tag{9}$$

$$s = \sqrt[n]{\frac{A^{n+1}}{r}} = (\mathrm{n}+1)\cdot\mathrm{r}\cdot\tau = \mathrm{A}\cdot\sqrt[\mathrm{n+1}]{(\mathrm{n}+1)\cdot\tau}, \tag{10}$$

$$A = \sqrt[n+1]{r\cdot s^n} = \frac{s}{\sqrt[n+1]{[(n+1)\cdot\tau]}} = [(n+1)\cdot\tau]^{\frac{n}{n+1}}\cdot r, \tag{11}$$

$$\tau = \frac{1}{n+1}\cdot\left(\frac{A}{r}\right)^{\frac{n+1}{n}} = \frac{1}{n+1}\cdot\left(\frac{s}{A}\right)^{n+1} = \frac{1}{(n+1)}\cdot\frac{s}{r}. \tag{12}$$

Referring to the kinematic aspect, the transversal acceleration and lateral jerk trends can be expressed by the following analytical relationships, which are also valid for $n=1$ [27]:

$$a_t = \frac{v^2}{r} = \frac{v^2}{A^{n+1}}\cdot s^n, \tag{13}$$

$$c = \frac{da_t}{dt} = v^3\cdot\frac{n}{A^{n+1}}\cdot s^{n-1}. \tag{14}$$

Regarding the rolling speed, the same considerations developed for the clothoid case apply.

3.3. Bloss Curve. The Bloss curve is a transition curve able to reduce the negative impacts due to geometric discontinuities at the start and end points of the junction. Its closed-form intrinsic equation is as follows [29]:

$$\frac{1}{r} = \frac{s^2}{\mathrm{RL}^2}\left(3-\frac{2s}{L}\right), \tag{15}$$

with obvious symbols meaning.

Analytically, this curve exhibits some similarities with multiparameter clothoids family (Equation (6)). In fact, Bloss curve intrinsic equation can be obtained by the difference of two GCS that have shape parameters n_1 and n_2 greater than unit ($n_1=2$ and $n_2=3$) and scale factors $A_1=(\frac{\mathrm{RL}^2}{3})^{1/3}$and $A_2=(\frac{\mathrm{RL}^3}{2})^{1/4}$, as shown in the following equations:

$$\frac{1}{r_1} = \frac{s^2}{A_1^3} = \frac{s^2}{\left(\frac{\mathrm{RL}^2}{3}\right)}, \tag{16}$$

$$\frac{1}{r_2} = \frac{s^3}{A_2^4} = \frac{s^3}{\left(\frac{\mathrm{RL}^3}{2}\right)}. \tag{17}$$

For this reason, the Bloss curve is also known as biparametric or bihyperclothoid [16].

From a kinematic point of view, the transversal acceleration and lateral jerk trends are characterized by the following analytical relationships:

$$a_t = \frac{v^2}{r} = \frac{v^2\cdot s^2}{\mathrm{RL}^2}\left(3-\frac{2s}{L}\right), \tag{18}$$

$$c = \frac{da_t}{dt} = v^3\cdot\frac{6s}{\mathrm{RL}^2}\cdot\left(1-\frac{s}{L}\right). \tag{19}$$

As for the rolling speed, nothing changes from the clothoid and multiparameter clothoid.

4. Case Studies and Kinematic Considerations

In this study, as mentioned above, the geometric and kinematic characteristics of six transition curves (one clothoid with a unitary "n" shape factor, four multiparameter clothoids with shape factors of 1.25, 1.50, 1.75 and 2.00, respectively, and the Bloss curve) were analyzed to assess their possible use in airport runways' RETs. Analyses were conducted for both runways with code numbers 1-2 and runways with code numbers 3-4, amounting to 12 case studies. The abovementioned transition curves were first examined individually and then compared with each other, both geometrically and kinematically.

The kinematic analyses were developed by MATLAB software calculating (https://matlab.mathworks.com/). In particular, the (realistic) hypothesis of uniformly decelerated motion regimen was adopted and a 0.001 m integration step was set along the planimetric reference elements development.

The analytical relationships described in the previous sections were used to calculate the uncompensated transversal acceleration and the lateral jerk along the development of the transition curves. The uncompensated transversal acceleration was calculated by the first relationship of Equations (4), (13), and (18) along constant curvature elements (circular curves). For lateral jerk calculation, instead, the first relationships of Equations (5), (14), and (19) and uniformly decelerated motion equations were applied, as shown in the following equation:

$$c = \frac{\frac{1}{r}\left(v_k^2 - v_{k-1}^2\right)}{\frac{v_k - v_{k-1}}{a}}, \tag{20}$$

where v_k and v_{k-1}, respectively, are the exit and inlet speeds in the considered section having a length of $\bar{l}$ (measured in m/s), a is the imposed constant deceleration (measured in m/s^2), and r is the circular curve radius, in meters.

In the first part of the study, kinematic evaluations were carried out starting from the ICAO impositions of exit velocities and decelerations (Section 2) [7].

Table 1: Main geometric parameters of the proposed RETs.

TC	CNs	SC (m)	TCL (m)	CCL (m)	SD (m)	TL (m)	FDA (g)	CCR (m)	SF (m)
Clothoid ($n = 1.00$)	1-2	128.45	60.00	185.99	35	280.99	6.94	275	0.55
GCS ($n = 1.25$)	1-2	121.38	63.10	187.94	35	286.04	6.49	275	0.55
GCS ($n = 1.50$)	1-2	117.25	66.42	189.41	35	290.83	6.15	275	0.55
GCS ($n = 1.75$)	1-2	115.14	70.01	190.52	35	295.53	5.89	275	0.55
GCS ($n = 2.00$)	1-2	114.40	73.79	191.39	35	300.18	5.69	275	0.55
Bloss curve	1-2	—	77.46	177.25	35	289.71	8.97	275	0.55
Clothoid ($n = 1.00$)	3-4	256.90	120.00	227.98	75	422.98	6.94	550	1.09
GCS ($n = 1.25$)	3-4	242.15	125.63	232.14	75	432.77	6.46	550	1.09
GCS ($n = 1.50$)	3-4	233.85	132.23	235.08	75	442.31	6.12	550	1.09
GCS ($n = 1.75$)	3-4	229.62	139.39	237.29	75	451.68	5.87	550	1.09
GCS ($n = 2.00$)	3-4	228.11	146.91	239.01	75	460.92	5.67	550	1.09
Bloss curve	3-4	—	154.27	210.85	75	440.12	8.93	550	1.09

Abbreviations: CCL, circular curve length; CCR, circular curve radius; CNs, code numbers; FDA, final deviation angle; SC, scale factor; SD, straight distance; SF, shift factor (offset); TC, transition curve; TCL, TC length; TL, total length.

After that, various deceleration values were investigated. In particular, the authors evaluated the possible use of deceleration values lower than the imposed limits. This was done in order to decrease the RETs travel time and thus to increase the runway capacity.

This study also verified the geometric and kinematic RETs effectiveness when exit speeds are higher than those fixed by ICAO (65 km/h for runway codes 1-2 and 93 km/h for runway codes 3-4, respectively). The main aim of this analysis is to make the RETs suitable even for larger aircraft, without having to provide for their expensive repositioning along the runway.

The speed "point by point" trend was calculated by applying the nonuniform motion law as described by the following relationship, with the obvious meaning of symbols:

$$v_k = \sqrt{v_{k-1}^2 - 2a\bar{l}}. \tag{21}$$

5. Geometrical Characterization of Case Studies

The RETs were designed starting from classical ICAO reference layouts (Figures 1 and 2). It was assumed that, from the starting point (positioned 30 or 60 m before the central exit curve's tangent point as function based on runway code), the pilot is tending to follow a variable curvature trajectory (clothoid-like) not drawn on the pavement.

According to this hypothesis and considering that the clothoid develops equally between the straight line and the circular curve [25, 27, 28], the authors imposed that its overall length should be equal to 60 m (runway codes 1-2) and 120 m (runway codes 3-4), respectively. This hypothesis causes offsets equal to 0.55 m for runway codes 1-2 and equal to 1.09 for runway codes 3-4.

The examined other transition curves were sized by imposing the same values of the clothoid offset, that is, 0.55 m for runway codes 1-2 and 1.09 m for runway codes 3-4. This assumption generated 10 other layouts characterized by reasonably different lengths of the transition curves and circular curves.

Numerical analyses have shown that if you increase the "n" shape parameter while the curvature radius is fixed, then the transition curve development increases and, simultaneously, both the scale factor "A" and the final deviation angle "τ_f" decrease.

Conversely, if the curvature radius redoubles from 275 m (runway codes 1-2) to 550 m (runway codes 3-4), then about twice the offsets, scale parameter "A" and planimetric development also double, while the final deviation angle remains almost constant.

Numerical analyses also showed that the Bloss curve's final deviation angle is greater than of the multiparameter clothoid with shape parameter "n" equal to 2. The overall planimetric development of RETs with an exit angle of 45° (runway codes 1-2) was on average 30% shorter than those with an exit angle equal to 30° (runway codes 3-4).

Table 1 shows the main geometric characteristics of both the proposed transition curves and complete exit junction elements.

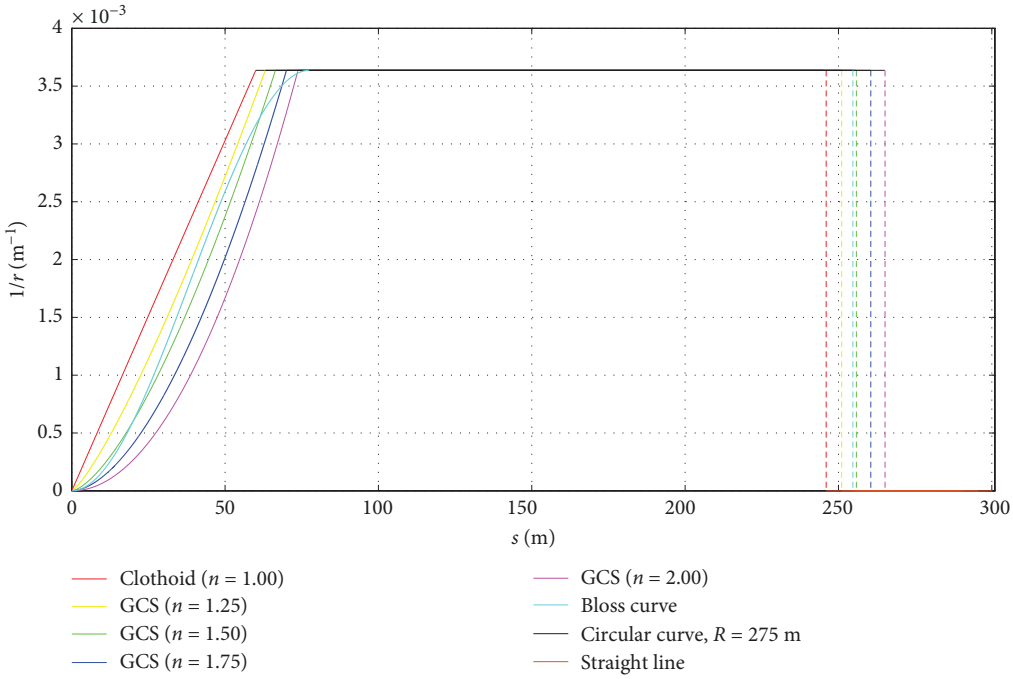

Figure 3: Curvature trend for runway codes 1-2.

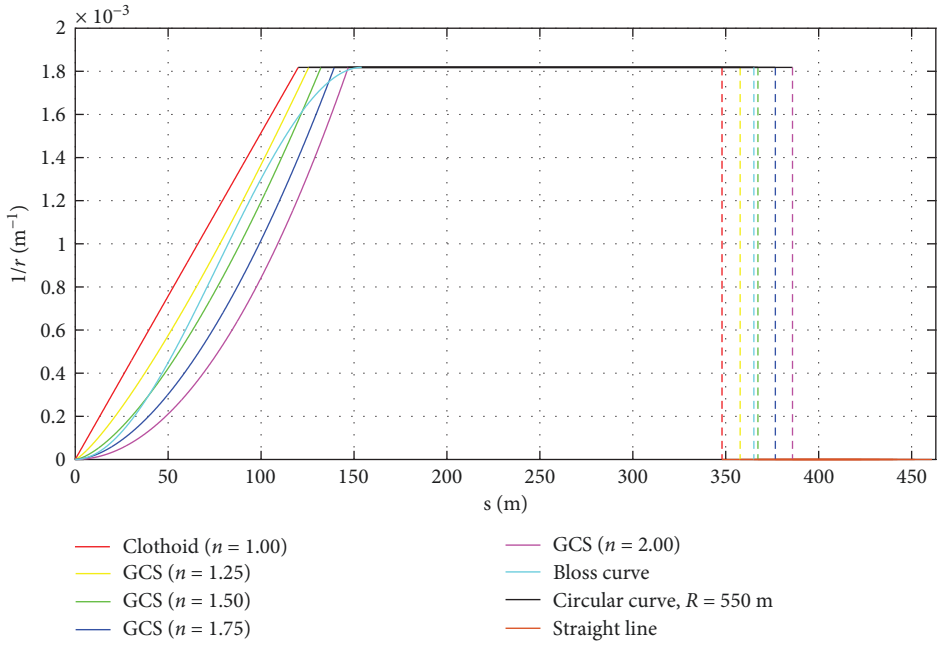

Figure 4: Curvature trend for runway codes 3-4.

6. Results and Discussion

In the following sections, the 12 case studies defined in this paper are analyzed and compared with each other. These case studies are analyzed with regard to curvature (Section 6.1), uncompensated transversal acceleration (Section 6.2), lateral jerk (Section 6.3), travel speed (Section 6.4), travel time (Section 6.5), longitudinal deceleration (Section 6.6), and centrifugal force (Section 6.7). The analyses were conducted by implementing the analytical relationships described in the previous sections.

6.1. Curvature. The curvature $1/r$ trend as a function of curvilinear abscissa for all examined RETs is shown in Figure 3 (runway codes 1-2) and Figure 4 (runway codes 3-4).

It can be noted that the multiparameter clothoids show a "smoother" trend than the clothoid, but that the better results are furnished by the Bloss curve because it does not show any

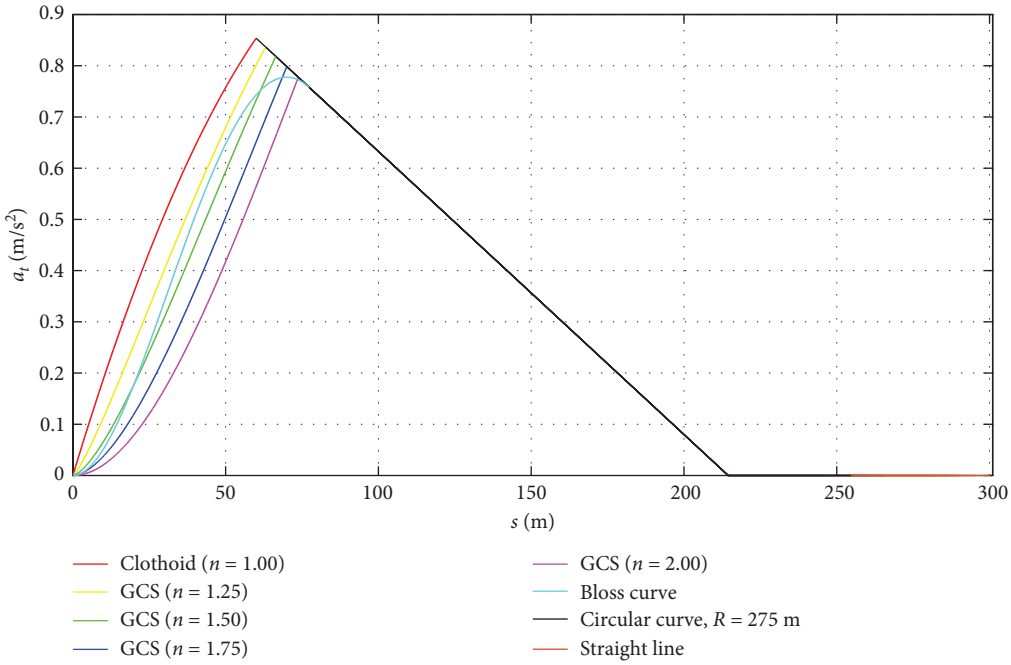

Figure 5: Uncompensated transversal acceleration trend for runway codes 1-2.

second-order discontinuity (angular point) in the passage between the transition element and the circular curve. The multiparameter clothoids exhibit a very comparable trend with each other, but they have obvious differences in development and curvature values, which are related to the different values of the shape parameter and scale factor.

All transition curves converge to the same maximum curvature value that is equal to 1/275 m^{-1} for runway codes 1-2 and it is equal to 1/550 m^{-1} for runway codes 3-4. These values remain constant along the entire circular arc development, until they reach zero at the straight line, after they have undergone a curvature discontinuity with a gap equal to 1/R.

6.2. Uncompensated Transversal Acceleration. Analysis results describing the a_t uncompensated transversal acceleration trend along curvilinear abscissa are shown in Figure 5 (runway codes 1-2) and Figure 6 (runway codes 3-4), respectively.

The diagrams describing the transversal acceleration trend along the clothoid and multiparameter clothoids are always continuous and increasing. The maximum values occur at the end point namely where the passage between the variable curvature element and the constant curvature element is achieved.

Next, these diagrams linearly decrease along the circular arc development, where the curves overlap. Obviously, for all examined curves, the transversal acceleration becomes zero along the entire straightway.

The clothoid is the transition curve showing the highest values of uncompensated transverse acceleration. At the passage point between the transition curve and the circular curve, the transversal acceleration percentage variation between the clothoid and multiparameter clothoid with shape parameter $n = 2$ is about 10%, for all runway codes. Specifically, it should be noted that doubling the shape parameter value from 1 (clothoid) to 2 (multiparameter clothoid) achieves a 9.81% decrease in maximum transversal acceleration for runway codes equal to 1-2 and 9.21% for runway codes of 3-4. The diagram describing the transversal acceleration trend in the Bloss curve lies somewhere between the two multiparameter clothoids having a shape parameter equal to 1.25 and 1.75, respectively. If runway code is equal to 3 or 4 (Figure 6), in the first 40 m of Bloss curve development (approximately 33% of the total length), the transversal acceleration value remains lower than shown by the GCS with $n = 1.5$.

Then, these values considerably increase and then they have the tendency to reach multiparameter clothoid values with $n = 1.25$. It can be seen that the multiparameter clothoid with $n = 2$ exhibits better performance than the Bloss curve because the transversal acceleration values are always lower along the total development.

The clothoid also shows an increasing trend of transversal acceleration as a function of curvilinear abscissa and exhibits a maximum value of 0.85 m/s^2 for runway codes 1-2 and 0.88 m/s^2 for runway codes 3-4. These values are on average about 9% greater than exhibited by the Bloss curve.

A comparison between the runways having a code numbers 1-2 (Figure 5) and 3-4 (Figure 6) shows that doubling the circular curve radius (from 275 to 550 m) causes an increase of about 3.26% of the maximum uncompensated transversal acceleration value for clothoid case study. For multiparameter clothoid with $n = 2$ and the Bloss curve, abovementioned increase is equal to 3.83% and 3.70%, respectively.

For runways having codes 3-4 (Figure 6), the transversal acceleration discontinuity between the circular curve and the straightway shows the highest value in the clothoid (0.25 m/s^2), while for the multiparameter clothoid with $n = 2$, the abovementioned discontinuity is about 40% lower.

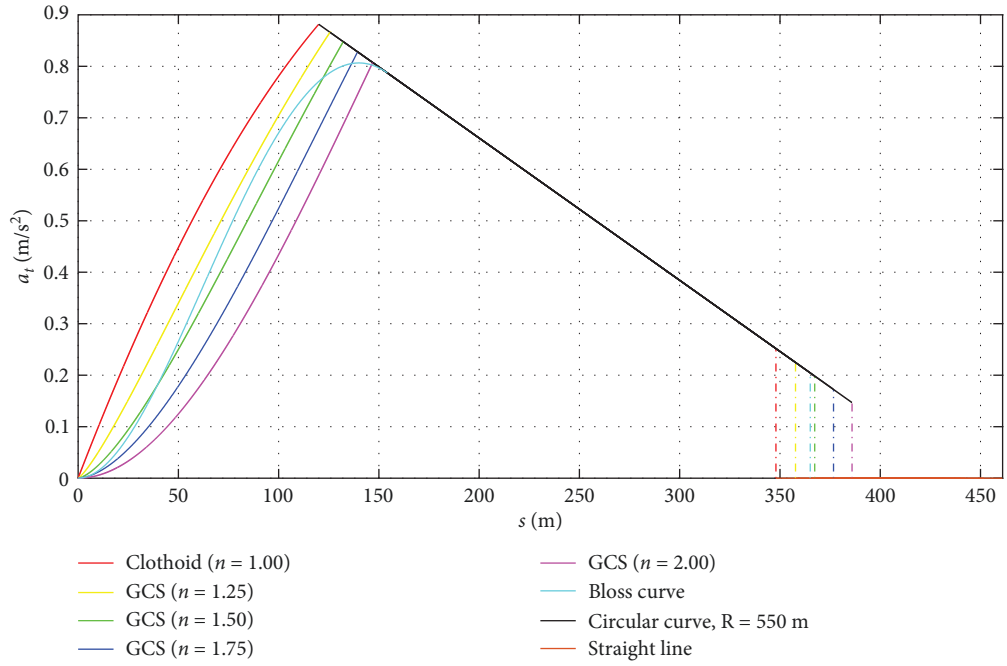

Figure 6: Uncompensated transversal acceleration trend for runway codes 3-4.

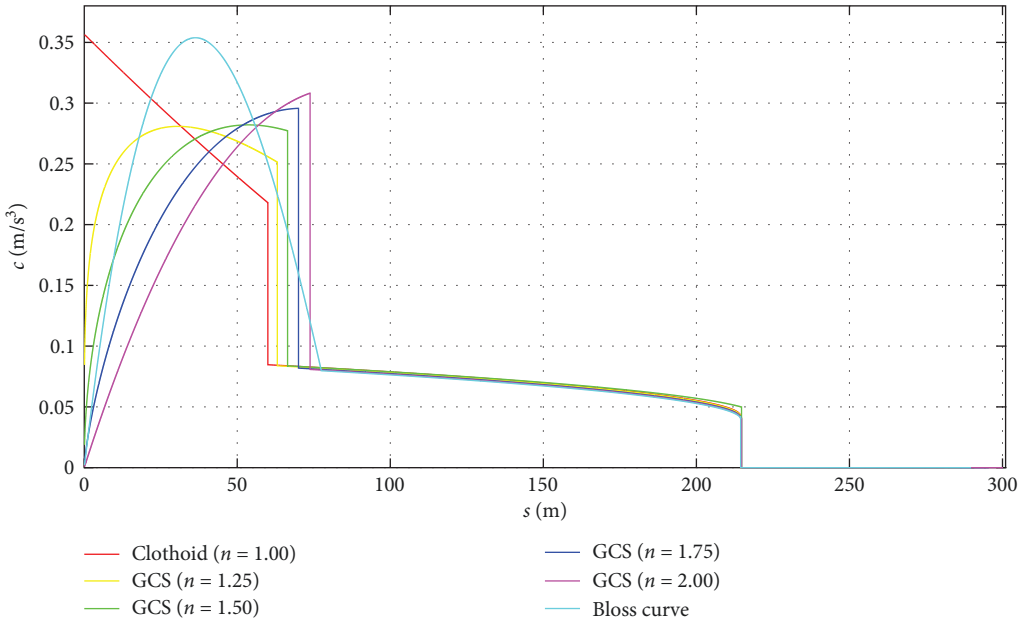

Figure 7: Lateral jerk trend for runway codes 1-2.

For runways having codes equal to 1 or 2 (Figure 5), there is no such discontinuity, because adopting the longitudinal deceleration values imposed by ICAO (Section 2), the aircraft stops within the circular curve without using the final straightway.

It is recommended that transversal acceleration should not exceed specific maximum values in order to ensure suitable comfort for passengers [30]. A generally accepted maximum physiological limit is 1.18 m/s^2 [31]. Obtained results show that abovementioned limit value is not exceeded in any of the proposed case studies.

6.3. Lateral Jerk. In Figure 7 (runway codes 1-2) and Figure 8 (runway codes 3-4), the c lateral jerk trend as a function of curvilinear abscissa is shown for all proposed RETs. Table 2 shows the maximum lateral jerk values (c_{max}) for each case study.

It can be noted that the lateral jerk value (at the same curvilinear abscissa) has lower values when increasing the

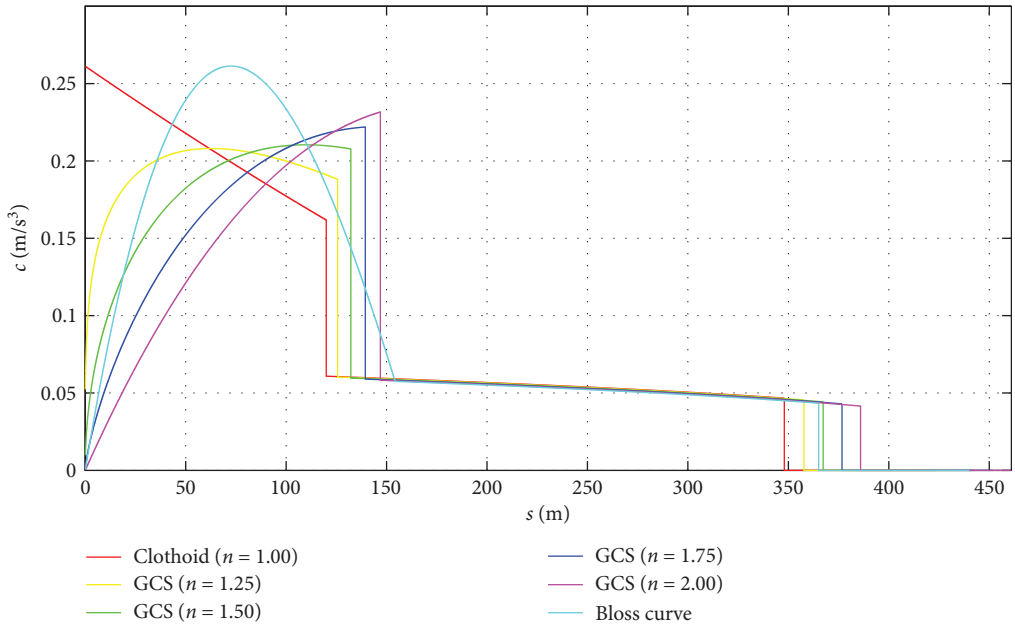

Figure 8: Lateral jerk trend for runway codes 3-4.

Table 2: Maximum lateral jerk value for each transition curve.

Transition curves	c_{max} (m/s^3) (runway codes 1-2)	c_{max} (m/s^3) (runway codes 3-4)
Clothoid	0.36	0.26
GCS ($n = 1.25$)	0.28	0.21
GCS ($n = 1.50$)	0.28	0.21
GCS ($n = 1.75$)	0.29	0.22
GCS ($n = 2.00$)	0.31	0.23
Bloss curve	0.35	0.26

"n" shape parameter and this is approximately in the first half of the transition curves development (Figures 7 and 8), namely in the most kinematically critical zone where the speeds are still sufficiently high. In this region, the GCS with shape parameter $n = 2$ shows the best performance, because the lateral jerk values are lower than those of the other curves.

Compared to the other transition curves, the clothoid is characterized by a high lateral jerk value at the initial point, equal to 0.36 m/s^3 for runway codes 1-2 and 0.26 m/s^3 for runway codes 3-4 (Figures 7 and 8 and Table 2). This significantly decreases passengers' comfort so it would be advisable to avoid the clothoid usage in the airport field, from this point of view.

On the other hand, the observed lateral jerk discontinuity at the passage point between the clothoid and the circular curve is the smallest compared to other transition curves. In particular, the "jump" is about equal to one-half of the exhibited "jump" by the multiparameter clothoid with $n = 2$.

The maximum lateral jerk value along the clothoid is similar to observed on the Bloss curve and it is about 14% and 12% larger (for runway codes 1-2 and 3-4, respectively) than of the observed value along multiparameter clothoid with $n = 2$ (Table 2). However, this comparison is not very significant. The most relevant aspect is the position where the peak value occurs.

This position is the absolute worst in the clothoid case, because it is located at the start of the transition curve, where the aircraft speeds are highest. The peak value in the Bloss curve occurs about in the middle of the transition curve, while in the multiparameter clothoid with $n = 2$, it occurs at the end of the transition curve, where the aircraft speeds are certainly lower.

With regard to the Bloss curve, it is observed that the lateral jerk trend is characterized by a bell-shaped curve. Thus, there is a first section where the lateral jerk increases from the nil value, on the starting point, to a specific maximum value. This value is located about in the midpoint curve and is equal to 0.35 m/s^3 for runway codes 1-2 and 0.26 m/s^3 for runway codes 3-4, respectively.

In the second part, the lateral jerk shows a decreasing trend, having "acceptable" values at end of the transition junction. Finally, the curve describing the lateral jerk trend joins to the circular curve, showing no geometric "discontinuity" (Figures 7 and 8 and Table 2). So, the Bloss curve compared with the other transition curves shows a more lateral jerk regular trend even though the maximum values are significantly higher than those of the other transition curves. However, as already abovementioned, these values occur in a better position than the clothoid, namely where aircraft speeds are sure to be lower (Section 6.4).

The lateral jerk values along the circular curve are very similar for all case studies, the most significant differences from each other are concentered along the transition curves. Comparing the runways of both code numbers 1-2 and code numbers 3-4, it could be observed that doubling the circular curve radius produces 26.76%, 24.85%, and 26.14% lateral jerk decrease for clothoid, multiparameter clothoid with $n = 2$ and Bloss curve, respectively.

It can be noted that the circular curve radius influence on the maximum transversal acceleration value (Section 6.2) is much smaller than the lateral jerk. Instead, the radius increase determines a large lateral jerk reduction and an increase in the transversal acceleration.

The international scientific literature provides several recommendations regarding maximum lateral jerk values. Generally, the maximum value of 1.3 ft/s^3 (0.396 m/s^3) is considered acceptable [1, 14]. Obtained results show that the maximum lateral jerk value is always lower than the specified threshold value.

The first phase of the kinematic analysis pointed out the limitations of using the clothoid and the greater effectiveness of the GCS with $n = 2$. In fact, this curve is already used in road design when vehicle speed is significantly variable. The Bloss curve also showed some kinematic advantages, in fact, the maximum value of the uncompensated transversal acceleration is always less than or similar to the values shown in the other case studies (Section 6.2, and Figures 5 and 6) with a lateral jerk trend always very smooth (bell-shaped curve). Although the maximum lateral jerk values along the Bloss curve are significantly higher than those of the other transition curves, they occur approximately in the transition curve middle, that is, in a better position than clothoid, where the aircraft speeds are lower (Section 6.3, and Figures 7 and 8).

6.4. Aircraft Ground Moving Speed. Based on the kinematic analysis, for each case studies, a speed analysis was conducted. This analysis was carried out for each transition curve following three approaches:

- Approach 1: runway exit speeds and longitudinal decelerations imposed by ICAO are used.
- Approach 2: runway exit speeds imposed by ICAO and longitudinal decelerations calculated by authors that allow the aircraft to stop exactly at the straight line end are used.
- Approach 3: runway exit speeds calculated by authors using longitudinal decelerations imposed by ICAO are used.

The obtained results referring to the most important case studies (clothoid, multiparameter clothoid with $n = 2$ and Bloss curve) are shown in Figure 9.

For diagram construction, the nonuniform motion law with imposed longitudinal deceleration was used. These diagrams show a decreasing trend which reaches the nil value at a variable position depending on the examined case study.

Each diagram analyzes three subcases. For runway codes 1-2 (Figure 9a,c,e), the first subcase (Approach 1) shows the RETs speed trend when the exit speed values (65 km/h) and longitudinal decelerations (0.76 m/s^2 on curves and 1.52 m/s^2 on straight lines) are those imposed by ICAO (Section 2). The second subcase (Approach 2) still considers the ICAO exit velocity (65 km/h) but sets a lower and constant deceleration along the RETs that allows the aircraft to stop exactly at the straight line end (0.58, 0.54, and 0.56 m/s^2 for the clothoid, GCS with $n = 2$ and Bloss curve, respectively). The third subcase (Approach 3) considers exit velocities greater than those set by ICAO. These speeds allow the aircraft to stop exactly at the end of the straight line (78.90, 81.25, and 79.98 km/h) with the longitudinal decelerations equal to those imposed by ICAO (0.76 m/s^2 on curves and 1.52 m/s^2 on straight lines).

For runway codes 3-4 (Figure 9b,d,f), the first subcase (Approach 1) shows the RETs speed trend when the exit speed values (93 km/h) and longitudinal decelerations (0.76 m/s^2 on curves and 1.52 m/s^2 on straight lines) are those imposed by ICAO (Section 2). The second subcase (Approach 2) still considers the ICAO exit velocity (93 km/h) and the ICAO deceleration along the curves (0.76 m/s^2) but sets a lower and constant deceleration along the straight line that allows the aircraft to stop exactly at the straight end (0.93, 0.54, and 0.75 m/s^2 for the clothoid, GCS with $n = 2$ and Bloss curve, respectively). The third subcase (Approach 3) considers exit velocities greater than those set by ICAO. These speeds allow the aircraft to stop exactly at the end of the straight line (99.04, 102.71, and 100.73 km/h) with the longitudinal decelerations equal to those imposed by ICAO (0.76 m/s^2 on curves and 1.52 m/s^2 on straight lines).

On runways having code numbers 3-4, the aircraft stops within the straightway at a different point for each case study (Figure 9b,d,f). Instead, on the runways having code numbers 1-2 the aircraft already stops within the circular curve before reaching the abovementioned straightway (Figure 9a, c,e).

This means that the maximum longitudinal deceleration limit values imposed by ICAO (Section 2) are very prudential and could reasonably be reduced/modified in order to use all available space. Table 3 shows the constant deceleration values used in Approach 2 along the examined layouts (Figure 9).

The lowest deceleration (0.54 m/s^2) is obtained for the GCS with $n = 2$ (runway codes 1-2) because this layout has the greatest overall development (Table 1), while the initial and final speeds are the same for all the analyzed layouts. Based on the identical considerations (lowest overall development), the clothoid exhibits the highest value of 0.58 m/s^2 (Tables 1 and 3).

For runways having code numbers equal to 3-4, it is not possible to use along the entirely transition junction a constant deceleration value lower than the ICAO recommended value because the available development is not adequate. For this reason, the authors have used the ICAO deceleration along the transition curve and the circular curve (0.76 m/s^2) and a lower value on the straight line. In this case, the straightway length remains unchanged (35 or 75 m based on runway codes).

The variable parameter is the aircraft speed at the initial point of abovementioned straightway, because both the transition elements developments and circular curves are dependent on the examined case study.

In fact, the multiparameter clothoid with $n = 2$ shows a lower deceleration value (0.54 m/s^2) because its overall development is higher (460.92 m), while the clothoid shows the highest deceleration value (0.93 m/s^2) because its overall development is lower (422.98 m).

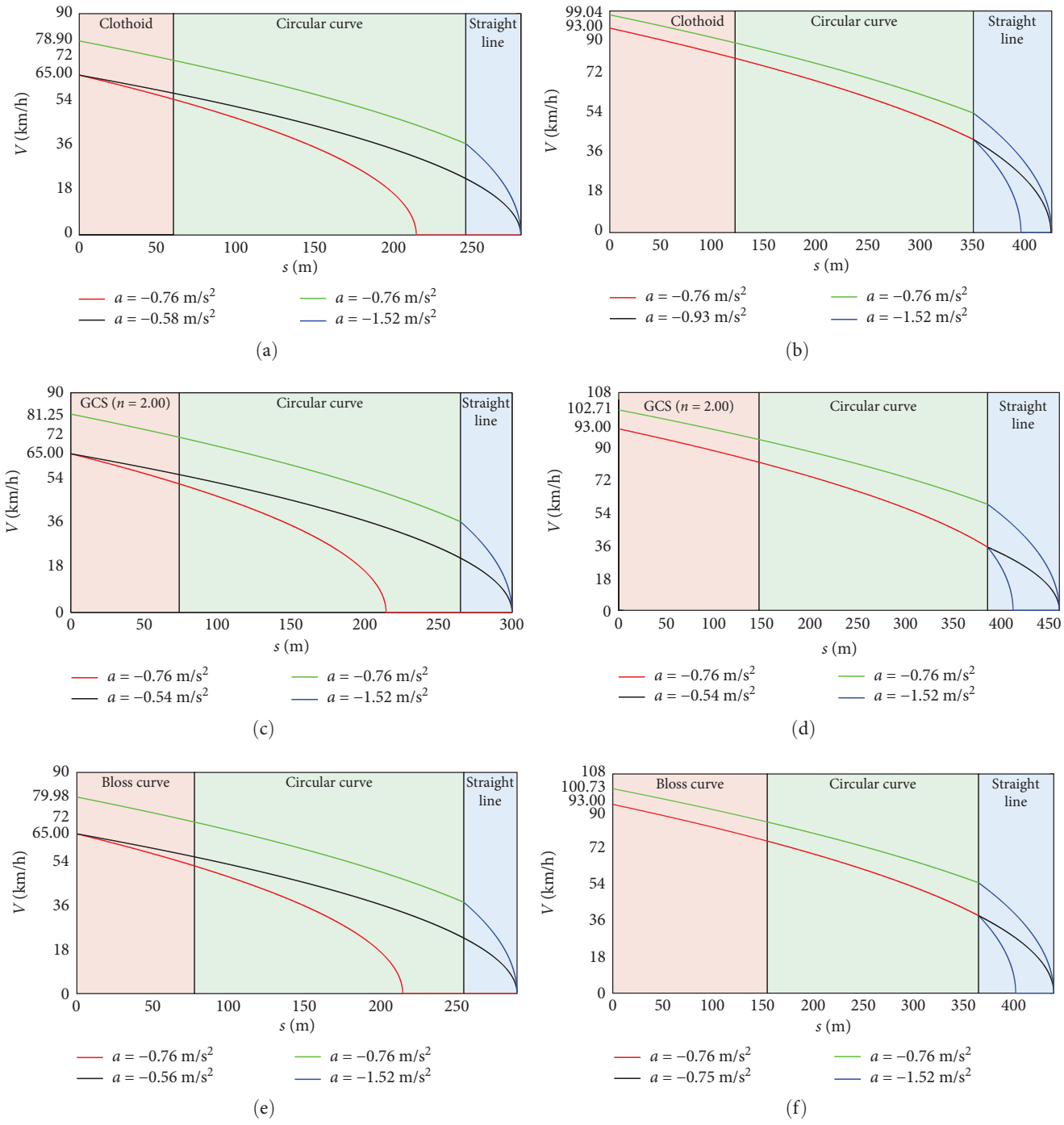

FIGURE 9: Longitudinal speed trend: (a) clothoid "1-2," (b) clothoid "3-4," (c) GCS $n = 2$ "1-2," (d) GCS $n = 2$ "3-4," (e) Bloss curve "1-2," and (f) Bloss curve "3-4".

Obtained results suggested to assess a new hypothesis (Approach 3), namely to keep the longitudinal deceleration values recommended by the ICAO, but to increase the runway exit speeds over the imposed maximum values (Figure 9 and Table 4). This is in order to use the overall available length.

However, this hypothesis requires greater care on the runways and RETs skid conditions. In fact, the new runway exit speeds need an increased transversal friction coefficient until 0.19 (Table 4), that is higher than the suggested ICAO maximum value equal to 0.13 (Section 3.1).

It is noted that, with regard to the runway codes 3-4, the maximum exit speed is achieved in the multiparameter clothoid with $n = 2$ (102.71 km/h) and that this speed is comparable with that of the other transition curves. For runways with code numbers 1-2 the speed increase, comparing to the

Table 3: Feasible decelerations for each case study (Approach 2).

Case studies	Runway codes 1-2, a (m/s^2)	Runway codes 3-4, a (m/s^2)
Clothoid	0.58	0.93
GCS ($n = 1.25$)	0.57	0.82
GCS ($n = 1.50$)	0.56	0.73
GCS ($n = 1.75$)	0.55	0.63
GCS ($n = 2.00$)	0.54	0.54
Bloss curve	0.56	0.75

Table 4: New runway exit speeds for each case study (Approach 3).

Case studies	Runway codes 1-2		Runway codes 3-4	
	V (km/h)	f_t	V (km/h)	f_t
Clothoid	78.90	0.18	99.04	0.14
GCS ($n = 1.25$)	79.52	0.18	100.01	0.14
GCS ($n = 1.50$)	80.11	0.18	100.95	0.15
GCS ($n = 1.75$)	80.69	0.19	100.86	0.15
GCS ($n = 2.00$)	81.25	0.19	102.71	0.15
Bloss curve	79.98	0.18	100.73	0.15

base value, is about 16 km/h and the maximum value equal to 81.25 km/h is again achieved along the multiparameter clothoid with $n = 2$.

The results show that the Bloss curve is the only transition that, even in the case of runway codes 3-4, allows aircraft to travel down the RETs without changing the value of longitudinal deceleration in the passage between the various elements of the exit (transition curve, circular curve, and straight line) and without changing the speed value from that imposed by ICAO (93 km/h). Figure 9f shows that the constant value of the longitudinal acceleration along the transition curve and the circular curve (0.76 m/s^2) is practically the same as that along the straight line (0.75 m/s^2) with evident advantages of comfort and driving regularity.

6.5. Travel Time. In order to reduce ROTs and expand airport capacity [32–34], the authors propose to increase runway exit speeds.

The impacts produced by increasing exit speeds (Section 6.4) can be investigated by analyzing aircrafts travel times in uniformly decelerated motion regimen. The abovementioned analysis was conducted according to three different approaches (Figure 9). This allowed three different time ranges to be calculated, as detailed below:

- Approach 1: Travel time calculation needs from the transition curve starting point to the point where the aircraft stops. Runway exit speeds and longitudinal decelerations suggested by ICAO (Section 2) are used.
- Approach 2: Travel time calculation needs from the transition curve starting point to the point where the RET ends. Runway exit speeds suggested by ICAO and longitudinal decelerations proposed by authors are used, respectively (Section 6.4 and Table 3).

Table 5: RETs travel times (runway codes 1-2).

Case studies	Approach 1 time (s)	Approach 2 time (s)	Approach 3 time (s)
Clothoid	23.75	31.13	22.05
GCS ($n = 1.25$)	23.75	31.69	22.28
GCS ($n = 1.50$)	23.75	32.21	22.50
GCS ($n = 1.75$)	23.75	32.74	22.71
GCS ($n = 2.00$)	23.75	33.25	22.90
Bloss curve	23.75	32.09	22.45

Table 6: RETs travel times (runway codes 3-4).

Case studies	Approach 1 time (s)	Approach 2 time (s)	Approach 3 time (s)
Clothoid	26.24	31.12	26.27
GCS ($n = 1.25$)	26.68	32.86	26.62
GCS ($n = 1.50$)	27.13	34.62	26.96
GCS ($n = 1.75$)	27.58	36.56	27.29
GCS ($n = 2.00$)	28.08	38.85	27.62
Bloss curve	27.02	34.18	26.88

- Approach 3: Travel time calculation needs from the transition curve starting point to the point where the RET ends. Runway exit speeds proposed by authors and longitudinal decelerations suggested by ICAO are used, respectively (Section 2).

Table 5 shows the obtained results for runways with code numbers 1-2.

It can be noted that using both runway exit speed values and deceleration values suggested by ICAO (Section 2), aircraft stop in 23.75 s, after traveling distance of about 215 m. This occurs for each case study but, it is an impractical solution because in this manner the aircrafts are unable to use the overall length of RETs (Approach 1). If the longitudinal decelerations proposed by the authors (Section 6.4) and the runway exit speeds imposed by ICAO (Section 2) are adopted, all aircrafts are able to complete the RETs overall length (Approach 2). Obviously, this requires a longer travel time, which is equal to 33.25 s in the multiparameter clothoid case with $n = 2$ (Table 5).

Finally, if the imposed ICAO decelerations (Section 2) and the runway exit speeds indicated by the authors (Section 6.4) are used, the travel times decreased about 10 s in comparison with the previous case (Approach 3). Again, the highest travel time is for the multiparameter clothoid with $n = 2$ (22.90 s). Such travel time is practically the same as that obtained in the other case studies (Table 5).

It can be observed that for runway codes 1-2, Approach 3 is the most effective one because it can generate an airport capacity increase, according to the furnished authors' indications. Similar considerations are valid for runway codes 3-4 (Table 6); although in this case, the aircraft stops at a specific point of the final straightway (Approach 1). This position is different according to the case study configuration (Section 6.4).

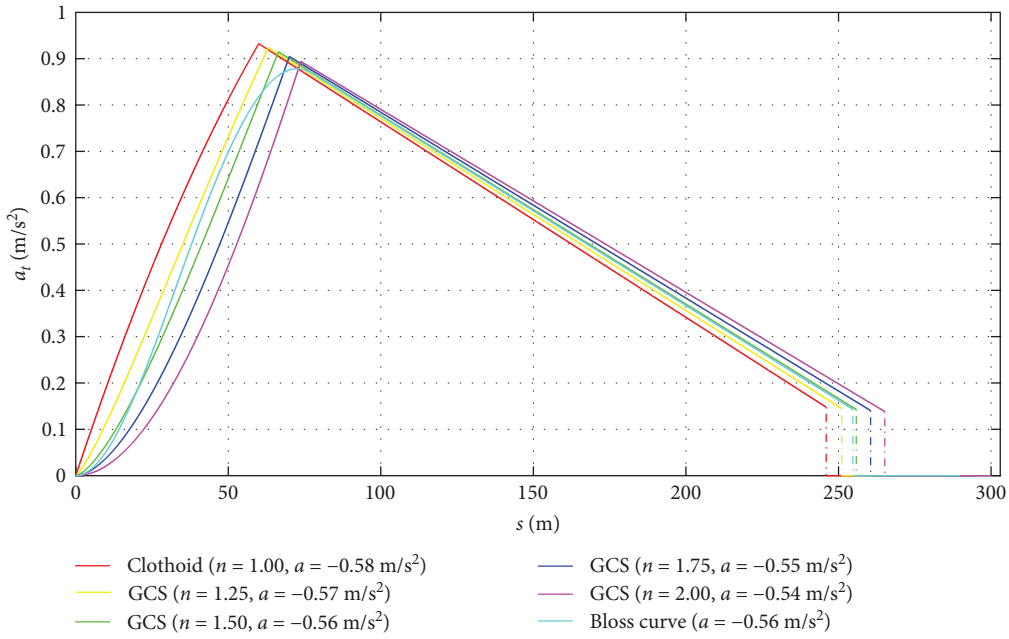

FIGURE 10: Transversal acceleration trend in case of imposed deceleration (runway codes 1-2).

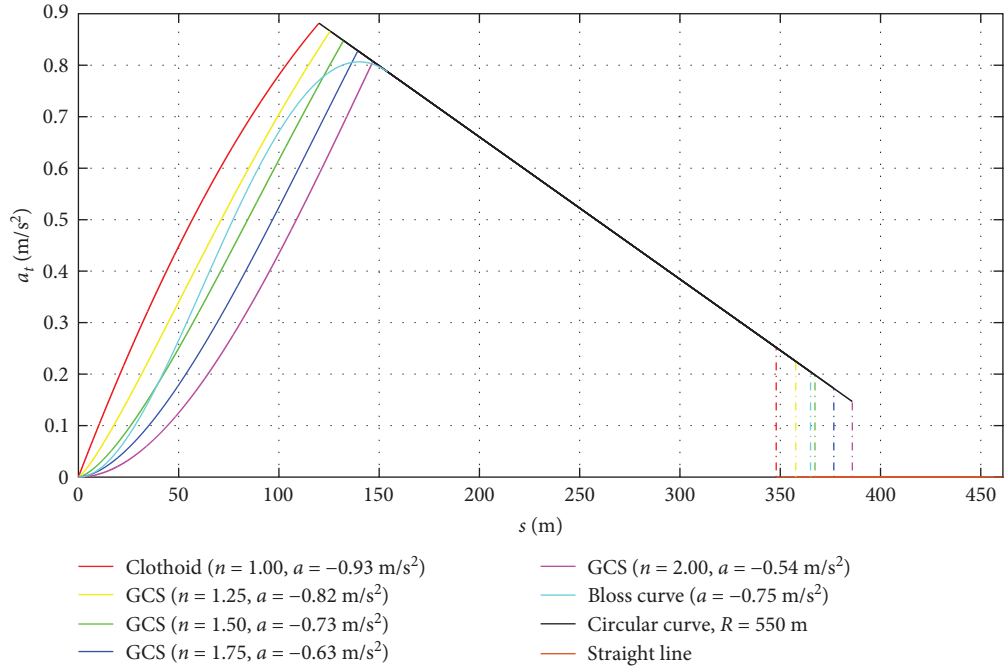

FIGURE 11: Transversal acceleration trend in case of imposed deceleration (runway codes 3-4).

As an example, for runway codes 3-4 and clothoid, the results obtained with each of the three approaches are described below (Section 6.4 and Table 6):

1. The aircraft exits from the runway at 93 km/h (25.83 m/s) and runs through the clothoid and circular curve at constant longitudinal deceleration of 0.76 m/s^2. At the end of the circular curve, its speed value is 11.77 m/s and it has spent a travel time of 18.50 s. Subsequently, the aircraft then keeps decelerating (1.52 m/s^2) and stops after traveling 45.57 m from the initial of the straightway, namely 393.54 m from the beginning of the taxiway, after a travel time of 7.74 s. There are 29.43 m of unused straightway length. The overall travel time is 26.24 s.
2. The aircraft turns at 93 km/h and runs through the clothoid and circular curve at constant longitudinal deceleration of 0.76 m/s^2 (for runway with code numbers

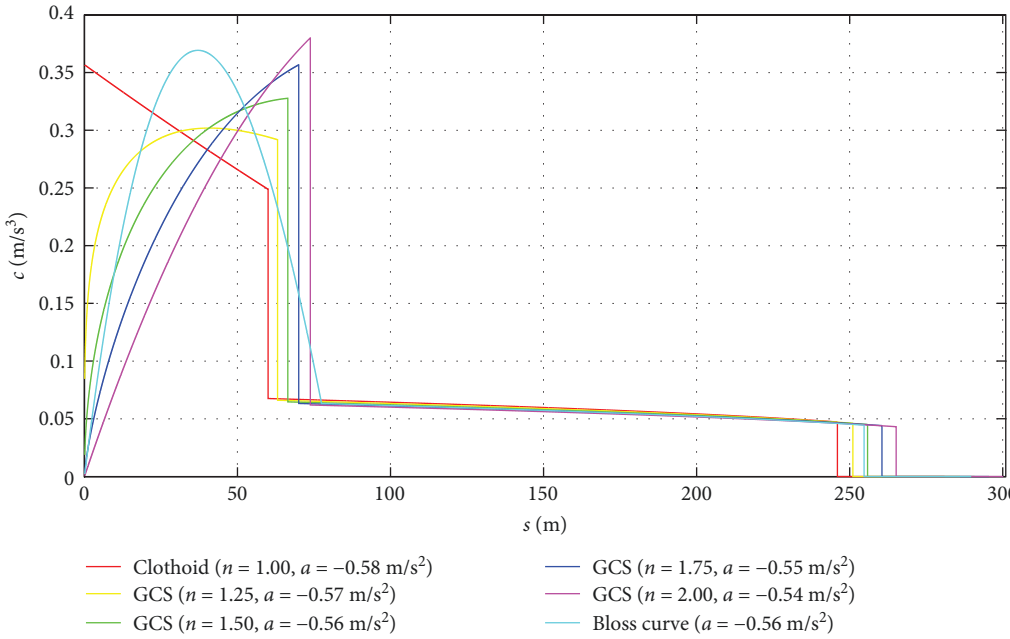

Figure 12: Lateral jerk trend in case of imposed deceleration (runway codes 1-2).

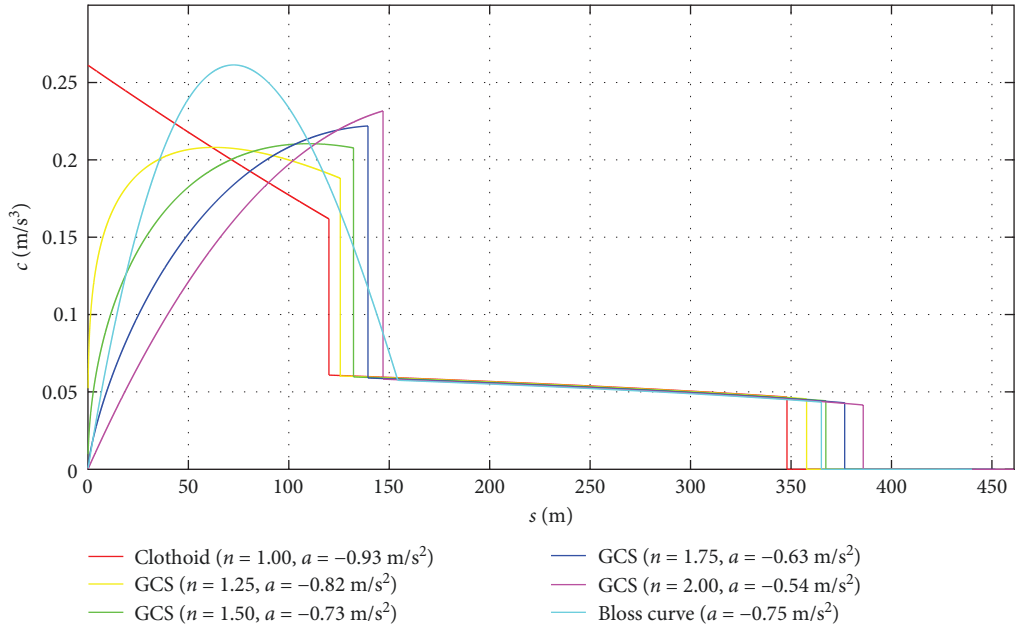

Figure 13: Lateral jerk trend in case of imposed deceleration (runway codes 3-4).

3-4, the proposed deceleration is used only along the final straight line). The speed value is 11.77 m/s at the end of the circular curve and the travel time is equal to 18.50 s (as in the previous case). After this, the aircraft keeps decelerating (0.93 m/s^2) and stops at the taxiway end, after a travel time of 12.62 s has passed. The total travel time is therefore 31.12 s.

3. The aircraft exits from the runway at 99.04 km/h (27.51 m/s) and runs through the clothoid and circular curve at constant longitudinal deceleration of 0.76 m/s^2. At the circular curve end, the speed value is 15.10 m/s and the travel time is 4.67 and 11.67 s, respectively. Thereafter, it keeps decelerating (1.52 m/s^2) and stops at the taxiway end in 9.93 s. The total travel time is therefore 26.27 s.

6.6. Deceleration Effects on Kinematic Variables. The motion regimen analysis for both runway codes 1-2 and 3-4 was developed by using the longitudinal deceleration values defined by the authors (Section 6.4 and Table 3). This is

in order to utilize entirely RETs length. Obtained results are shown in Figures 10–13.

This causes higher both transversal acceleration and speed values than obtained in the previous analysis (Sections 6.2 and 6.4). The more detailed analysis shows a peak transversal acceleration increase equal to 9.19% for the clothoid, equal to 14.98% for the multiparameter clothoid with $n = 2$, and equal to 12.93% for the Bloss curve. The lateral jerk increase is 23.29% and 4.35% for the multiparameter clothoid with $n = 2$ and for the Bloss curve, respectively, while there is no increase for the clothoid. This is because the maximum lateral jerk value occurs at the initial section of the transition curve, where speed has not changed (65 km/h) and therefore has not been any effect due to the deceleration decrease. Moreover, it can be noted that using an average deceleration of 24% less than the ICAO imposed threshold values causes a speed increase so that, even in the runways with code numbers 1-2, the aircraft has to use the final straightway to stop. Unlike previously, the aircraft does not end its run in the circular curve, so that a discontinuity at the passage to the final straightway is evident in the diagrams (Figures 10 and 12).

It can be seen that despite the benefits produced by speed increase (RETs travel time decrease), the deceleration decrease causes both a transversal acceleration and lateral jerk increase. However, it is noted that these increments are still conservative compared to the imposed limits (Sections 6.2 and 6.3).

6.7. Centrifugal Force. As well-known, the centrifugal force value acting on aircraft in curves is proportional both to the transversal acceleration and aircraft mass. Thus, for a qualitative analysis purpose, it can be observed that if a unitary mass value is assigned to the aircraft, the unit centrifugal force (UCF) trend along the design RETs coincides exactly with transversal acceleration. This means that the UCF peak value (UCF_{max}) occurs in the passage from the transition curve end point to circular curve beginning point (Figures 5 and 6).

If transition curves are lacking, the UCF's peak value at the circular curve beginning is equal to 1.18 m/s^2 for runways with code numbers 1-2 ($V = 65$ km/h, $R = 275$ m) and 1.21 m/s^2 for runways with code numbers 3-4 ($V = 93$ km/h, $R = 550$ m), respectively.

The analysis results show that the transition curves implementation in the design RETs produces an UCF percentage decrease (ΔUCF_{max}) averagely equal to 30% (Table 7). For both multiparameter clothoid with $n = 2$ and Bloss curve, this reduction reaches the maximum value of about 34%.

It can be emphasized that in the first part of the RETs where the speed values are particularly high, for the same aircraft mass, each of the proposed curves generates a lower centrifugal force respect conventional layouts due to a low curvature value. Instead, in the second half of RETs, the high variation of centrifugal force depends on both aircraft mass and high curvature value.

With reference to the obtained results, it can be affirmed that the use of the proposed transition curves generally results in beneficial stress decrease on aircraft gears.

Table 7: Maximum unit centrifugal force (UCF_{max}) and UCF percentage decrease (ΔUCF_{max}).

Case studies	UCF_{max} (m/s^2) (Runways codes 1-2)	ΔUCF_{max} (%) (Runways codes 1-2)	UCF_{max} (m/s^2) (Runways codes 3-4)	ΔUCF_{max} (%) (Runways codes 3-4)
Clothoid	0.85	−27.97	0.88	−27.27
GCS ($n = 1.25$)	0.84	−28.81	0.87	−28.10
GCS ($n = 1.50$)	0.82	−30.51	0.85	−29.75
GCS ($n = 1.75$)	0.80	−32.20	0.83	−31.40
GCS ($n = 2.00$)	0.78	−33.90	0.81	−33.06
Bloss curve	0.78	−33.90	0.81	−33.06

7. Conclusions

7.1. Detailed Conclusions. This study highlighted that the RETs geometric layouts as provided by ICAO need to be updated in order to make them more efficient and comfortable. Obtained results confirmed the clothoid inadequacy to be used as a transition curve in the RETs due to the instantaneous lateral jerk changes occurring at its initial point.

In fact, this point is characterized by significantly higher speeds and transversal acceleration values that are significantly higher than those generated by the multiparameter clothoids and the Bloss Curve. With reference to multiparameter clothoids, the study showed that as the shape parameter "n" increases, the lateral jerk significantly decreases.

In particular, it was observed that the layout which provides the highest safety level and comfort is the multiparameter clothoid with a shape parameter $n = 2$. The main advantages of using multiparameter clothoid over the clothoid are to ensure a lower lateral jerk value at initial point and a greater aircraft lateral stability.

Bloss curves also showed many advantages in terms of safety and travel comfort. Although the Bloss curve is characterized by a maximum lateral jerk value that is comparable to clothoid, it does not occur at its starting point, but rather at a significantly more advantageous position. Moreover, the Bloss curve does not exhibit any lateral jerk's geometric "jump" in the passage between the transition curve and the circular curve. Anyway, regarding the uncompensated transversal acceleration, the multiparameter clothoids with a shape parameters equal to 1.75 and 2.00 show better performance than the Bloss curve and significantly better performance than the clothoid.

With reference to lateral jerk, it can be observed that the peculiar bell curve shape that characterizes the Bloss curve is sure to be more effective than the increasing trend that characterizes multiparameter clothoids and that places the maximum value at the transition curve end. Conversely, the multiparameter clothoid with $n = 2$ ensures the lowest lateral jerk values within the first half of its development. Anyware, both transversal acceleration and lateral jerk are always under threshold limits indicated in the international scientific literature.

The study also analyzed the use of lower longitudinal deceleration values than those imposed by ICAO (i.e., higher exit speeds) in order to utilize all available space, decrease travel time, and increase airport capacity.

Analyses have shown that the maximum decelerations imposed are conservative because they induce the stopping aircraft within the curve, namely before the final straightway (code numbers 1-2).

The final phase of this study focused on the qualitative analysis of the dynamic stress acting on aircrafts. In particular, it was observed that the use of a transition curve, such as the multiparameter clothoid with $n = 2$ or the Bloss curve, can help to reduce shear stresses on the aircraft landing gears' shock absorber. As a matter of fact, obtained results showed that using of transition curves generates a UCF average decrease equal to about 30%. It should be noted that the principal aim of this work is to increase the capacity of existing airports with minimally invasive actions limited only to the geometric design of RETs, without providing for their repositioning along runways (Section 1). This is to minimize the retrofitting costs of conventional RETs designed by ICAO and/or FAA standards. From a qualitative point of view, the increase in construction cost of a traditional RET compared with a new RET with transition curve included is proportional to the variation in overall length if the cross-section layout is the same. In this meaning, it is observed that for runway codes 1-2, the length increases of traditional RET compared to the one with GCS ($n = 2.00$) and the one with Bloss curve is equal to 6.8% and 3.1%, respectively, while for runway codes 3-4, it is 9.0% and 4.0%, respectively (Table 1). These length increases (that are proportional to construction cost increase) are certainly not excessive, but to evaluate the effectiveness of the project, they must be compared with the benefits generated by the increased runway capacity. This analysis represents the level of investigation that will be developed by the authors in the second phase of this research.

In conclusion, the study showed that the multiparameter clothoid with shape parameter $n = 2$ and the Bloss curve are most suitable geometrical curves to be used as transition curves in airport RETs. Compared with existing ICAO and FAA layouts, they better solve the problem of aircrafts curve entrance when speeds are extremely variable. It is noted that further improvement and suggestions may be derived by the use of swept path analysis software. They make it possible to simulate vehicles and aircraft ground pathways and are currently widely used in the field of road engineering [35].

It is the authors' hope that the results obtained from this research, and subsequent in-depth studies, will be adopted by major government agencies such as the ICAO and the FAA. This means that existing or future standards should include the possibility of using RETs consisting of multiparameter clothoids with shape parameter $n = 2.00$ and/or Bloss curves. This is the case both in the construction of new airports and in the existing airports retrofitting.

The benefits are clear from a geometric, kinematic, and dynamic point of view, as well as for increasing airport capacity. The proposed modifications do not require moving RETs along the existing airport runways but only geometric retrofitting.

7.2. General Conclusions. In this study, the authors described the use of some variable radius transition curves in airport runway RETs. Twelve case studies were analyzed (six for runways with code numbers 1-2 and six for runways with code numbers 3-4). These case studies were defined starting from the two ICAO layouts, which are composed of a circular arc and a final straightway, as is well-known.

In fact, it can be observed that the aircraft pathway along the RETs contains a variable curvature element (clothoid-like). For this reason, the authors hypothesized the presence of a clothoid before the circular curve allowing a gradual transition between the runway and the RET. In particularly, the study evaluated the possible use of multiparameter clothoids (GCS) with shape parameters equal to 1.25, 1.50, 1.75, and 2.00 and the Bloss curve.

The analytical processing was developed "point by point" by MATLAB software because the outgoing aircraft motion regimen is uniformly decelerated. Results comparative analysis was done regarding curvature, transversal acceleration, lateral jerk, travel speed, travel time, longitudinal deceleration, and centrifugal force. The study showed that classical ICAO layouts of RETs are inadequate regarding safety and travel comfort, so they need to be revised using appropriate transition curves. Obtained results indicated considerable use possibilities both multiparameter clothoid with $n = 2$ and the Bloss curve.

The use of abovementioned transition curves also makes it possible to increase the runways capacity without having to plan and implement expensive RETs displacements.

Data Availability Statement

Data are included within the manuscript.

Conflicts of Interest

The authors declare no conflicts of interest.

Author Contributions

All authors contributed equally to this work. All authors have read and agreed to the published version of the manuscript.

Funding

There aren't financially supporting bodies.

References

[1] R. Horonjeff, F. X. McKelvey, W. J. Sproule, and S. B. Young, "Planning & Design of Airports," (Mc Graw Hill (2010).

[2] Airports Council International (ACI World), "What to Expect: Latest Air Travel Outlook Reveals Short- and Long-Term Demand," 2024, https://aci.aero/2023/02/22/what-to-expect-latest-air-travel-outlook-reveals-short-and-long-term-demand.

[3] International Civil Aviation Organization (ICAO), "Safe Skies. Sustainable Future," 2024, URL: https://www.icao.int.

[4] Federal Aviation Administration (FAA), "Providing the Safest, Most Efficient Aerospace System in the World," 2024, URL: https://www.faa.gov.

[5] A. A. Trani, A. G. Hebeika, B. J. Kim, V. Nunna, and C. Zhong, "Runway Exit Designs for Capacity Improvement Demonstrations. Phase II-Computer Model Development,"

(Virginia Polytechnic Institute and State University, Center for Transportation Research, Virginia (1992).
[6] N. P. Meijers and R. J. Hansman, "Data-Driven Predictive Analytics of Runway Occupancy Time for Improved Capacity at Airports," in *Report No ICAT-2019-14, MIT International Center for Air Transportation (ICAT)*, (Massachusetts Institute of Technology, Cambridge (USA), 2019).
[7] International Civil Aviation Organization (ICAO), "Doc 9157: Aerodrome Design Manual. Taxiways, Aprons and Holding Bays," International Civil Aviation Organization, Fifth Edition, 2020).
[8] Federal Aviation Administration, "Formulation of the National Plan of Integrated Airport Systems (NPIAS) and the Airports Capital Improvement Plan (ACIP)," *FAA Order* 5090, no. 5 (2019).
[9] L. L. Green, "Analysis of Runway Incursion Data," (NASA Langley Research Center, Hampton, Virginia (2013).
[10] S. Galagedera, H. R. Pasindu, and V. Adikariwattage, "Evaluation of the impact of runway characteristics on veer-off risk at rapid exit taxiways," *Transportation Research Interdisciplinary Perspectives* 12 (2021): 100480.
[11] N. Distefano and S. Leonardi, "Aircraft Runway Excursion Features: A Multiple Correspondence Analysis," *Aircraft Engineering and Aerospace Technology* 91, no. 1 (2018): 197–203.
[12] F. M. La Camera, "Il Calcolo del Progetto Stradale-La Planimetria," (Masson-ESA, Second edition, 1992): 88–405-3234-x.
[13] R. Horonjeff, D. M. Finch, D. M. Belmont, and G. Ahlborn, *Exit Taxiway Location and Design", Report prepared for the Airways Modernization Board by the Institute of Transportation and Traffic Engineering* (Berkeley: University of California, 1958).
[14] A. A. Trani, A. G. Hebeika, H. D. Sherali, B. J. Kim, and C. K. Sadam, "Runway Exit Designs for Capacity Improvement Demonstrations Phase I- Algorithm Development," (Virginia Polytechnic Institute and State University, Center for Transportation Research, Virginia (1990).
[15] A. Kobryń, "Transition Curves for Highway Geometric Design," in *Springer Tracts on Transportation and Traffic*, 14, (Springer International, Publishing.
[16] M. Agostinacchio, "La Curva Biparametrica Quale Raccordo Planimetrico Stradale a Gradiente di Curvatura Progressivo," *Autostrade* 3 (1983): 26–35.
[17] T. F. Brustad and R. Dalmo, "Railway Transition Curves: A Review of the State-of-the-Art and Future Research," *Infrastructures* 5, no. 5 (2020): 43.
[18] K. Zboinski and P. Woznica, "Is the Cubic Parabola Really the Best Railway Transition Curve?" *Open Engineering* 11, no. 1 (2021): 1207–1213.
[19] A. Basak, "The Study of Geometry of the Selected Transition Curves in the Design of Circular Roads," in *Advances in Science and Technology Research Journal*, 16, no. 4, (ISSN, 2022): 270–278.
[20] International Civil Aviation Organization (ICAO), "Annex 14: Aerodromes-Aerodrome Design and Operations," 1 (2022), International Civil Aviation Organization.
[21] Federal Aviation Administration (FAA), "AC 150/5300-13B: Airport Design," (2022).
[22] Federal Aviation Administration (FAA), "AC 150/5300-13B: Airport Design," (1989).
[23] D. Ciampa and S. Olita, "The Use of Bloss Curve in the Exit Lanes of Road Intersections," in *The Baltic Journal of Road and Bridge Engineering*, 15, (ISSN, 2020): 76–102.
[24] Ministero delle Infrastrutture e dei Trasporti (MIT), "Norme Funzionali e Geometriche per la Costruzione Delle Strade," no. 3 (2002).
[25] M. Agostinacchio, D. Ciampa, and S. Olita, "Strade Ferrovie Aeroporti," in *EPC Libri*, (Roma, ISBN, Fourth edition, 2024).
[26] P. Di Mascio, L. Domenichini, and A. Ranzo, "Infrastrutture Aeroportuali," (Efesto, Third edition, 2016).
[27] F. Giannini, F. La Camera, and A. Marchionna, "Appunti di Costruzione di Strade Ferrovie ed Aeroporti per il Corso di Laurea in Ingegneria Civile Trasporti," (Masson-ESA (1993).
[28] M. Agostinacchio, D. Ciampa, and S. Olita, "La Progettazione Delle Strade," in *EPC Libri*, (Roma, ISBN, Second edition, 2011).
[29] A. Bloss, "Der Ubergangsbogen mit Geschwungener Uberhohungsrampe," *Organ fur die Fortschritte des Eisenbahnwesens* 73, no. 15 (1936).
[30] S. P. Deligianni, M. Quddus, A. Morris, A. Anvuur, and S. Reed, "Analyzing and Modeling Drivers' Deceleration Behavior From Normal Driving," *Transportation Research Record* 2663, no. 1 (2017): 134–141.
[31] K. N. de Winkel, T. Irmak, R. Happee, and B. Shyrokau, "Standards for Passenger Comfort in Automated Vehicles: Acceleration and Jerk," *Applied Ergonomics* 106, no. N (2023): 103881.
[32] A. A. Trani, J. Cao, and M. Tarragò, "Limited Study of Flight Simulation Evaluation of High-Speed Runway Exits," *Transportation Research Record* 1066, no. 1 (1999): 82–89.
[33] F. Maltinti, M. Flore, F. Pigozzi, and M. Coni, "Optimizing Airport Runway Capacity and Sustainability Through the Introduction of Rapid Exit Taxiways: A Case Study," *Sustainability* 16, no. 13 (2024): 5359.
[34] P. D. Mascio, G. Rappoli, and L. Moretti, "Analytical Method for Calculating Sustainable Airport Capacity," *Sustainability* 12, no. 21 (2020): 9239.
[35] D. Ciampa, M. Diomedi, F. Giglio, S. Olita, U. Petruccelli, and C. Restaino, "Effectiveness of Unconventional Roundabouts in the Design of Suburban Intersections," *European Transport/ Trasporti Europei* 80 (2020): 1825–3997.